SPC

Advanced Journal of Chemistry-Section A

Journal homepage: www.ajchem-a.com

Original Research Article

Molecular Structure, FT-IR Spectra, MEP and HOMO-LUMO Investigation of 2-(4-Fluorophenyl)-5-phenyl-1, 3,4-oxadiazole Using DFT Theory Calculations

Sunil Laxman Dhonnar[1] *, Nutan Vitthal Sadgir[1], Vishnu Ashok Adole[2], Bapu Sonu Jagdale[2]

[1] *Department of Chemistry, L.V.H. Arts, Science, and Commerce College, Panchavati, Nashik, India*
[2] *Department of Chemistry, Arts, Science, and Commerce College, Manmad, Nashik, India*

ARTICLE INFO

Article history

Submitted: 24 April 2021
Revised: 12 May 2021
Accepted: 17 May 2021
Available online: 20 May 2021
Manuscript ID: AJCA-2104-1254

DOI: 10.22034/AJCA.2021.283003.1254

KEYWORDS

DFT
FT-IR
HOMO-LUMO
MESP

ABSTRACT

In the present work, synthesis and DFT study of 2-(4-fluorophenyl)-5-phenyl-1,3,4-oxadiazole is reported. The 6-311++G (d,p) basis set was used to optimize the molecular structure of the title compound using the DFT/B3LYP method. The structural parameters, bond length, and bond angle were studied. The fundamental vibrational wavenumbers and intensities were computed, and the observed and calculated wavenumbers were found to be in excellent agreement. In order to decide the reactivity and possible site for electrophilic and nucleophilic, Frontier molecular orbital (HOMO-LUMO) energies, global reactivity descriptors, molecular electrostatic potential as well as Mulliken charges were calculated using the same theory. The obtained results indicates that the compound possess good kinetic stability. The molecular electrostatic potential surface analysis shows that the nitrogen atom oxadiazole ring is the binding site for electrophilic attack.

* Corresponding author: Dhonnar, Sunil L.
✉ E-mail: sunildhonnar@gmail.com

GRAPHICAL ABSTRACT

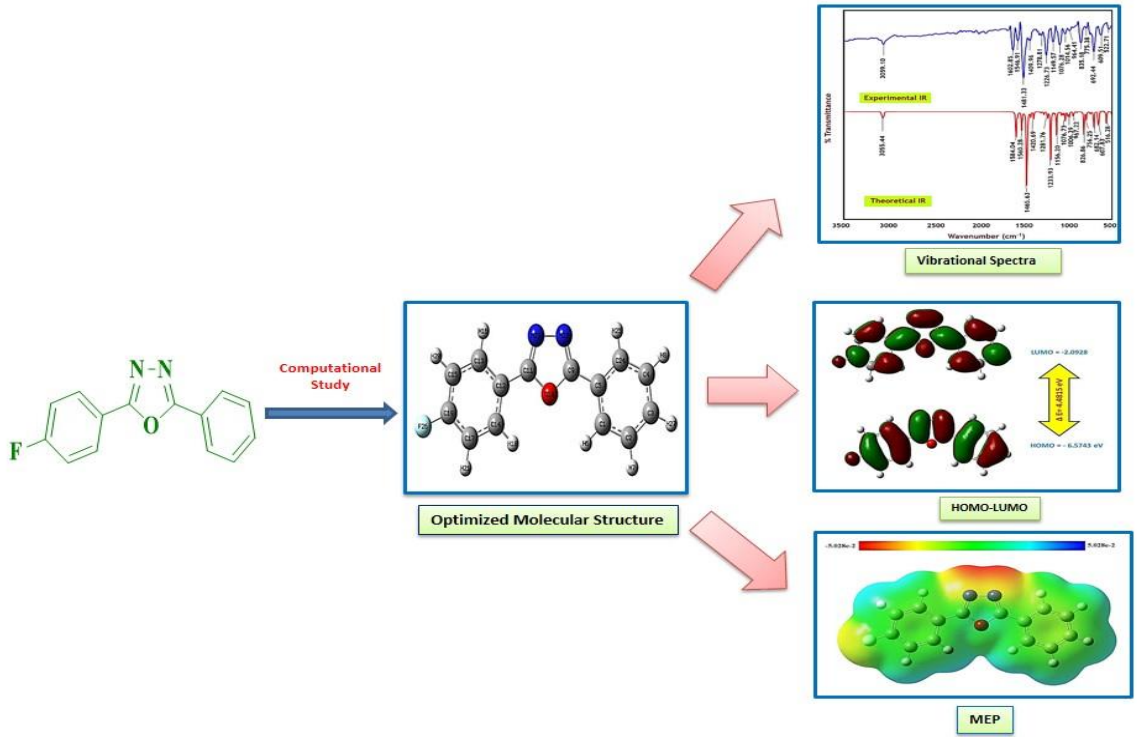

Introduction

Due to various remarkable biological and pharmacological properties, 1,3,4-oxadiazoles ($C_2H_2N_2O$) their noteworthy class of compounds have long piqued interest. Antitubercular [1], antimicrobial [2-3], anticancer [4], anti-inflammatory [5], anticonvulsant [6], analgesic [7], and insecticidal activities [8] are some of the prominent pharmacological applications of 1,3,4-oxadiazoles. Computational chemistry has recently drawn attention among researchers and scientists as a means of solving real problems in chemical, medicinal, biotechnology, and material science [9,11]. Computational chemistry is used in the designing of new drugs and materials to solve numerical problems [9,12-14]. Nowadays, resarchers use various computational programs to predict the molecular structure and physical properties of bioactive molecules [11-13]. The density functional theory (DFT) is a popular method for defining the structural and electronic properties of atoms and molecules [10,11] . The B3LYP functional and 6-311++G(d,p) basis set have been found to be the most typically used level of theory for DFT simulations in order to analyze various optical, spectral, and charge density properties of large and small molecules [15-17]. Many organic systems' vibrational spectra have been calculated using DFT, and the findings have shown to be encouraging. [18,20]. Molecular electrostatic potential (MESP) is commonly used as a reactivity map to explain hydrogen bonding interactions, as well as sites for electrophilic and nucleophilic reactions on organic molecules [21]. Very few reports have addressed theoretical computation of the 1,3,4-oxadiazole deivatives. This study presented a good tool to assess the theoretical insights into these biologically active compounds and thereby researchers can explore the molecular and spectroscopic properties. It has been reported

that the B3LYP functional with 6- 311++G(d,p) basis set provides good agreement between the theoretical and experimental structural and spectroscopic data [8,16]. Therefore, in the present investigation, we employed the B3LYP functional with 6- 311++G(d,p) basis set for the investigation of stuctural and spectroscopic facets of the titled compound. As far as our knowledge goes, the theoretical and experimental (FT -IR, HOMO-LUMO) study of 2-(4-fluorophenyl)-5-phenyl-1,3,4-oxadiazole has not been reported. Therefore, in continuation of our research in the field of therotical study of organic componds [22-25], here we wish to report DFT study of 2-(4-fluorophenyl)-5-phenyl-1,3,4-oxadiazole. The DFT study was used to enlighten the theoretical determination of the optimized molecular geometries, HOMO-LUMO energy gap, MEP, chemical reactivity, and stability of the title compound by using DFT/ B3LYP method with 6- 311++G(d,p) basis set.

Experimental details

Physical measurements

Melting point was measured by using open capillary method and uncorrected. The FT-IR spectrum was measured at room temperature on the Schimadzu spectrometer in the region of 4000-400 cm^{-1}. All chemicals were purchased from commercial suppliers.

Synthesis 2-(4-fluorophenyl)-5-phenyl-1, 3, 4-oxadiazole (FPPO)

4-Fluorobenzohydrazide (0.002 moles) with benzoic acid (0.002 moles) was dissolved in dry phosphorous oxychloride. The reaction mixture was then refluxed for 3 hours. The reaction mixture was then concentrated using a rotatory evaporator, and the resulting residue was quenched with ice water. The solid separated was filtered off, washed with water, and purified further by recrystallization with isopropanol to yield the 2-(4-fluorophenyl)-5-phenyl-1,3,4-oxadiazole as a white crystalline solid. The synthetic method and structure of the title compound are shown in Scheme 1.

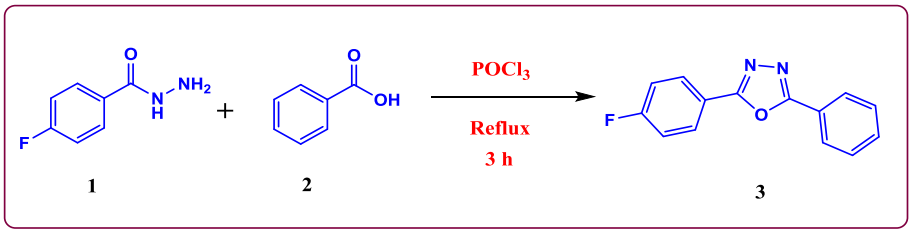

Scheme 1. Synthesis of 2-(4-fluorophenyl)-5-phenyl-1,3,4-oxadiazole

Computational details

The Gaussian 03 software [26] was used to perform all calculations. The optimized geometrical parameters and vibrational frequencies of the compound were calculated using the DFT/ B3LYP [27,28] method and the basis set 6-311G++(d,p). To maintain equilibrium between empirical and theoretical harmonic frequencies, the scale factor 0.9613 [29] was used. The findings were analyzed with the aid of the gauss view 4.1 molecular visualisation software [30]. DFT method with the same basis set has been put forth for calculating Molecular electrostatic potential, Mulliken charges, electronic properties such as HOMO-LUMO energies and reactivity parameters.

Results and Discussion

Molecular geometry

All DFT calculations were performed in gas phase. Table 1 shows the relevant structural

parameters of title molecule (FPPO) which have been obtained by DFT. The optimize structure of the FPPO molecule with the labeling of atoms are shown in Figure 1. No symmetry constraint has been noticed during geometry optimization. The molecular structure of the title FPPO molecule contains two phenyl rings attached to central oxadiazole core ring. The Para-fluoro substituted phenyl ring considered as PhI and unsubstituted ring attach to C9 carbon of central oxadiazole ring that is considered as PhII. The C-O bond length oxadiazole structures were found between 1.368 Å-1.366 Å. The C19-F26, C11-C12 and C9-C5 bond lengths are 1.352 Å, 1.456Å and 1.457 Å, respectively, and found within the normal range. The optimized structure is found to be with C1 point group symmetry having its ground state energy of -823.67845783 a.u. If the dihedral angles between three rings are analyzed, we can see that they are on the same plane. The bond lengths of C11-N23 and C9-N22 bond is 1.298, showing a double bond character. The optimized bond length of in six member ring PhI is calculated in the range 1.402–1.386 Å, whereas it is slightly greater for another six membered ring PhII and found in the range 1.403–1.389 Å. In optimized structure, phenyl C-H bond lengths are observed within the range 1.083–1.084 Å.

Table 1. Some selected structural parameters of FPPO molecule calculated by DFT/B3LYP/6-311++G (d,p) methods

Connectivity	Bond Length [Å]	Connectivity	Bond Angle [°]	Connectivity	Dihedral Angel [°]
C1-C2	1.392	C1-C5-C24	119.66	C5-C1-C2-C3	0.0006
C1-C5	1.401	C1-C2-C3	120.22	C5-C1-C2-H7	180.00
C1-H6	1.083	C1-C2-H7	119.67	H6-C1-C2-C3	179.99
C2-C3	1.394	C1-C5-C9	121.18	H6-C1-C2-H7	-0.0002
C2-H7	1.084	C2-C3-H27	120.07	C2-C1-C5-C9	-180.00
C3-C4	1.396	C2-C1-H6	120.16	C2-C1-C5-C24	-0.0005
C3-H27	1.084	C2-C3-C4	119.7	H6-C1-C5-C9	-0.0021
C4-H8	1.084	C3-C2-H7	120.11	H6-C1-C5-C24	180.004
C5-C9	1.457	C3-C4-H8	120.05	C1-C2-C3-C4	-0.0004
C5-C24	1.403	C3-C4-C24	120.31	C1-C2-C3-H27	-179.99
C9-O10	1.368	C4-C24-C5	119.93	H7-C2-C3-C4	179.99
C9-N22	1.298	C4-C24-H25	120.92	H7-C2-C3-H27	0.0005
O10-C11	1.366	C4-C3-H27	120.06	C2-C3-C4-H8	-179.99
C11-N23	1.298	C5-C9-O10	119.72	C2-C3-C4-C24	0.001
C11-C12	1.456	C5-C1-H6	119.83	H27-C3-C4-H8	-0.001
C12-C13	1.402	C5-C24-H25	119.14	H27-C3-C4-C24	179.99
C12-C14	1.401	C5-C9-N22	128.63	C3-C4-C24-C5	0.000
C13-C15	1.388	C9-N22-N23	106.87	C3-C4-C24-H25	180.00
C13-H16	1.083	C9-O10-C11	102.91	H8-C4-C24-C5	180.00
C14-C17	1.391	C9-C5-C24	119.16	H8-C4-C24-H25	0.0009
C14-H18	1.082	O10-C11-C12	119.74	C1-C5-C9-O10	-0.0261
C15-C19	1.388	O10-C11-N23	111.76	C1-C5-C9-N22	180.00
C15-H20	1.083	O10-C9-N22	111.64	C24-C5-C9-O10	179.97
C17-C19	1.386	C11-C12-C13	119.15	C24-C5-C9-N22	0.0037
C17-H21	1.083	C11-C12-C14	121.31	C1-C5-C24-C4	0.0002
C19-F26	1.352	C11-N23-N22	106.80	C1-C5-C24-H25	179.99
N22-N23	1.386	C12-C13-H16	119.19	C9-C5-C24-C4	-179.99
C24-H25	1.083	C12-C14-H18	119.92	C9-C5-C24-H25	0.0018
C4-C24	1.389	C17-C19-F26	118.79	C5-C9-O10-C11	-179.98

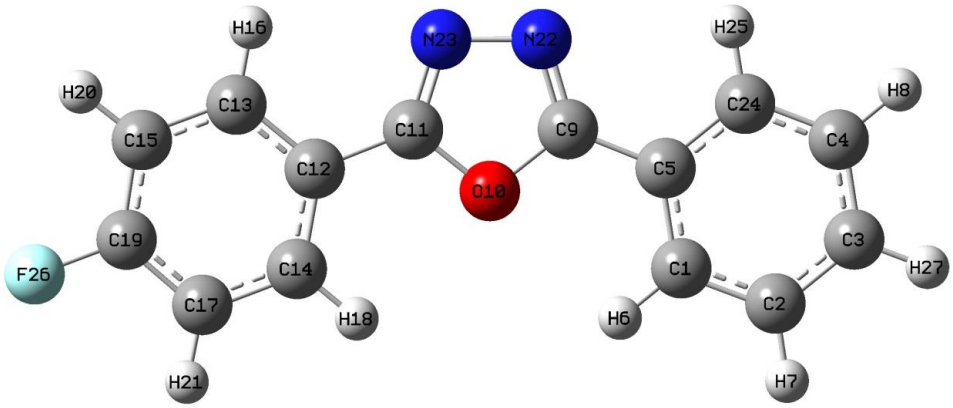

Figure 1. The molecular structures of FPPO molecule obtained by DFT/B3LYP/6-311G++ (d,p) method

Vibrational frequency assignment

Experimental IR spectrum is recorded in the region of 4000-500 cm^{-1} (Solid phase) and calculated vibrational spectrum in the gas phase. The title FPPO molecule contains total 27 atoms with 75 fundamental modes of vibration. Theoretical and experimental IR spectrum is shown in Figure 2. Table 2 shows some of the theoretical and experimental vibrations with intensity and their assignments. The stretching vibrations of the aromatic C-H ring are usually located between 3100 and 3000 cm^{-1}. The C-H stretching vibrations of the title molecule are assigned to the measured frequencies in the range 3085-3045 cm^{-1}. The experimental vibrational frequency appears in the range 3059 cm^{-1} of the IR spectrum showing good correlation with calculated frequency 3055 cm^{-1}. The In-plane C-H bending vibrations for aromatic ring is experimentally observed at 1481,1409, 1278,1149,1076,1014 cm^{-1}, showing good correlation with computed vibrations at 1465,1420,1281,1156,1076,1006 cm^{-1}. Similarly, the out of plane vibrations for aryl rings observed at 964,835,775,692 cm^{-1} agreed with computed 967,826,756,682 cm^{-1} infrared vibrations. The identification of C=N stretching frequencies was a rather difficult task because of the mixing of vibrations. The C=C and C=N mixed stretching modes experimentally were observed at 1602, 1546 and 1481 cm^{-1} and by DFT method it was observed at 1584, 1560 and 1465 cm^{-1}. In the fingerprint region of the FT-IR spectrum the C-O stretching vibration mode were observed at frequencies 1226 and 1149 cm^{-1}, calculated at 1233 and 1156 cm^{-1}, respectively. These vibrations are coupled with C-C in-plane bending modes and vibrations in the in-plane bending mode. The bands attributable to C-F stretching vibrations can be found in the vibrational spectra of the FPPO molecule over a broad frequency range of 1360-1000 cm^{-1}. In this study, the C-F stretching mode of vibration for FPPO was determined to be 1197 cm^{-1}, but this band was not observed experimentally.

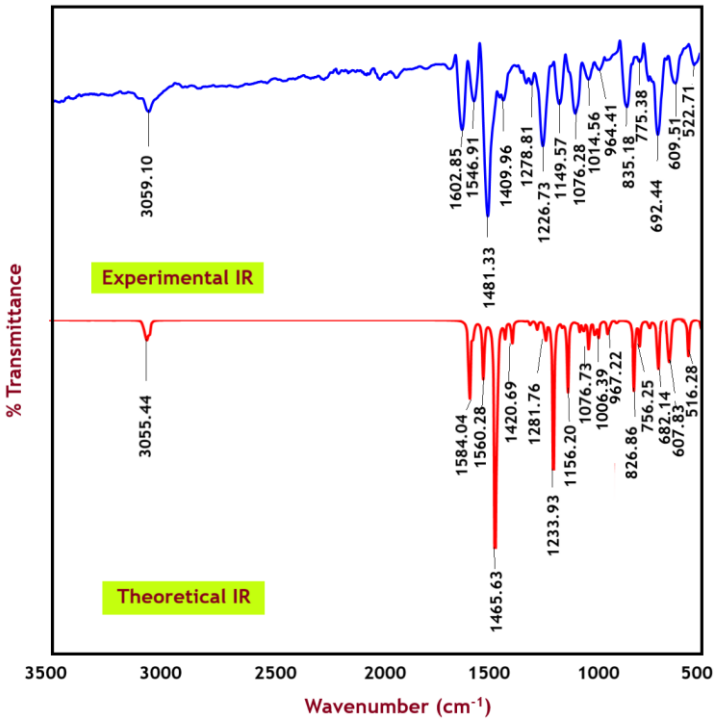

Figure 2. Experimental and Theoretical IR spectrum of FPPO molecule

Table 2. The observed FT-IR and calculated (B3LYP/6-311++G level) frequencies along with their selected assignments of the FPPO molecule

Mode	Theoretical Wavenumbers Scaled (cm^{-1})	Intensity	Experimental Wavenumbers (cm^{-1})	Assignment
75	3085.77	2.7190	-	υ sym. CH PhI
74	3084.33	0.6382	-	υ sym. CH PhI
73	3079.37	3.8333	-	υ sym. CH PhII
72	3075.22	5.5976	-	υ sym. CH PhII
71	3073.79	0.2556	-	υ asym. CH PhI
70	3071.41	3.2309	-	υ asym. CH PhI
69	3065.55	16.761	-	υ asym. CH PhII
68	3055.44	8.5716	3059	υ asym. CH PhII
67	3045.80	0.3449	-	υ asym. CH PhII
66	1584.04	76.358	1602	υ C=C + υ C=N
63	1560.28	2.9180	1546	υ C=C + υ C=N
60	1465.63	211.97	1481	υ C=C + υ C=N + β CH PhI
58	1420.69	12.601	1409	β CH PhII
54	1281.76	0.3858	1278	β CH PhI & PhII
51	1233.93	19.620	1226	υ C11-C12 + υ C9-C5 + υ COC
50	1197.47	133.25	-	υ C-F + β CH PhI
49	1156.20	3.6979	1149	υ COC + β CH PhI & PhII
45	1076.73	7.8148	1076	β CH PhI
42	1006.39	15.678	1014	υ N-N + β CH PhII
41	992.28	4.0500	-	υ N-N
38	967.22	0.0854	964	ρ CH PhII

31	826.87	43.7954	835	ρ CH PhII
27	756.25	7.4313	775	ρ CH PhI
24	682.14	27.733	692	ρ CH PhII & I
20	607.83	2.0777	609	Γ CCCC
18	516.28	6.5654	522	β C11-C12 + β C9-C5

υ - stretching; asym-asymmetric; sym-symmetric; def-deformation; β-in-plane bending; γ-out of plane bending, Γ- torsion, oxa-oxadiazole ring

Frontier molecular orbitals and Global Chemical Reactivity Descriptors

Descriptors of global reactivity are used to forecast global reactivity patterns. Frontier molecular orbitals are the highest occupied and lowest unoccupied molecular orbitals, respectively. Figure 3 shows a HOMO-LUMO plot of the title compound (FPPO). The calculated HOMO and LUMO energies in the gas phase are -6.5743 eV and - 2.0928 eV, respectively. The energy gap of the title compound, on the other hand, is 4.4815 eV. Various chemical reactivity parameters were calculated using the HOMO-LUMO energies. The HOMO represents the outermost orbital filled by electrons and is directly related to the ionization potential while the LUMO can be thought as the first empty innermost orbital unfilled by electron and is directly related to the electron affinity. Using Koopmans' theorem and equations 1-4, The parameters ionisation potential (I), electron affinity (A), chemical hardness (η), and chemical softness (S), electronic chemical potential (μ) as well as global electrophilicity index (ω) were calculated [31-35].

$$\eta = ½ (I - A) \quad (1)$$

$$S = 1/\eta \quad (2)$$

$$\mu = -½ (I+A) \quad (3)$$

$$\omega = \mu^2 / 2\eta \quad (4)$$

The frontier molecular energy gap aids in determining the molecule's chemical reactivity and stability. Table 3 shows HOMO, LUMO energies and global reactivity parameters, the global hardness (η) of 2.2407 eV, Chemical Softness (S) 0.4462 eV, electrophilicity Index (ω) 4.1904 eV, chemical potential (μ) - 4.3335 eV. Compaired with previously published literature [36-40], these calculated results indicated that the compound possess good kinetic stability.

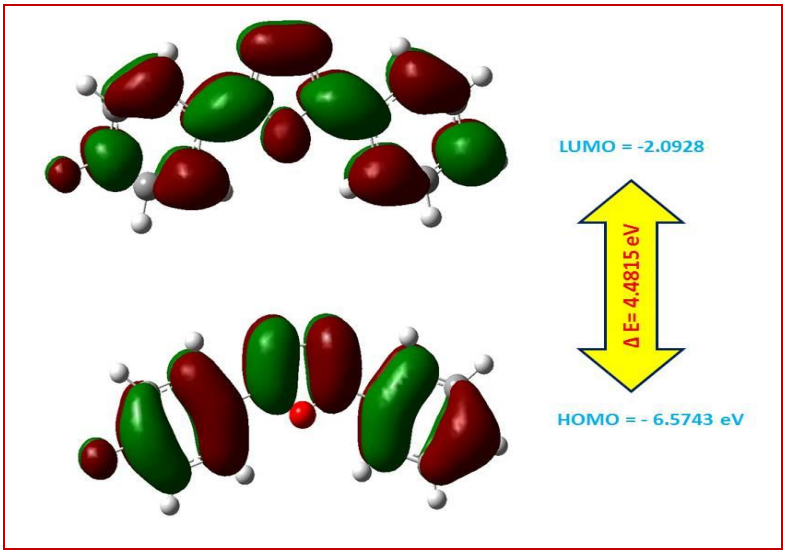

Figure 3. Frontier molecular orbitals surface and energy gap for FPPO Molecule

Table 3. The HOMO-LUMO energys and reactivity descriptor values of the FPPO Molecule are computed in the gas phase

Parameters	B3LYP/6-311++G(d,p)
E_{LUMO} (eV)	- 2.0928
E_{HOMO} (eV)	- 6.5743
$\Delta E = E_{LUMO} - E_{HOMO}$ (eV)	4.4815
Electron affinity **A**	2.0928
Ionization Energy **I**	6.5743
Global Hardness **η** (eV)	2.2407
Chemical Softness **S** $(eV)^{-1}$	0.4462
Electronic chemical potential **μ** (eV)	- 4.3335
Global electrophilicity Index **ω** (eV)	4.1904

Mulliken atomic charges and molecular electrostatic potential

Mulliken atomic charges are useful in determining the chemical reactivity of compounds. Table 4 presents the Mulliken atomic charges of various atoms in the title molecule. The C12 and C5 atoms, as shown in Table 4, have the highest positive charge of all carbon atoms and are thus predicted to be the target of nucleophilic attack on the title compound. Of all carbon atoms, the C4 and C14 atoms have a higher negative charge. The atoms of oxygen, nitrogen, and fluorine have a negative charge. Hydrogen atoms all have a positive charge.

Table 4. Mulliken atomic charges at the B3LYP/6-311++G (d, p) level for the title compound

Atom	Charge	Atom	Charge
1 C	-0.519	15 C	-0.151
2 C	-0.219	16 H	0.230
3 C	-0.234	17 C	0.197
4 C	-0.604	18 H	0.149
5 C	0.816	19 C	-0.594
6 H	0.135	20 H	0.204
7 H	0.183	21 H	0.211
8 H	0.172	22 N	-0.002
9 C	-0.148	23 N	-0.033
10 O	-0.005	24 C	0.002
11 C	-0.004	25 H	0.226
12 C	0.926	26 F	-0.168
13 C	-0.253	27 H	0.162
14 C	-0.685		

The molecular electrostatic potential surface (MESP) plot is a representation of electrostatic potential plotted on a constant electron density surface. The chemical reactivity of sites is determined by the molecular electrostatic potential. The polar nature of the title compound (FPPO) is indicated by its dipole moment of 3.3514 Debye. The MESP method was used to predict the presence of reactive sites in the FPPO molecule for electrophilic and nucleophilic attack. MESP for the title compound are shown in Figure 4. Different colours on the MESP plot reflect different electrostatic potential values: Red, blue, and green regions represent maximum electrophilic reactivity, nucleophilic reactivity, and zero electrostatic potential, respectively. Decrease in potential occurs as blue > green > yellow > orange > red. The MESP of the title

molecule clearly demonstrates the presence of a large negative potential area around nitrogen atoms, which is coloured red, and where electrophilic attack can occur. The hydrogen atoms have the most positive electrostatic potential, while the rest of the molecule appears to be almost neutral.

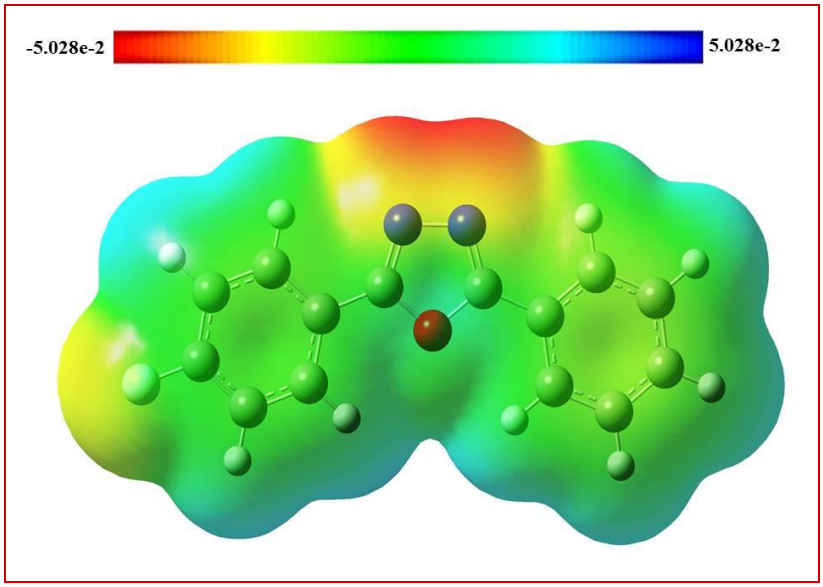

Figure 4. The MESP map of the title compound (FPPO)

Conclusion

In this paper, we conducted an experimental and theoretical vibrational study of 2-(4-fluorophenyl)-5-phenyl-1,3,4-oxadiazole. The DFT (B3LYP) system 6-311++G(d,p) basis set was used to determine the molecular geometry parameters and wavenumbers (Vibration spectra) for the title compound in the ground state. The experimental vibrational frequencies were found to be in strong agreement with the measured vibrational frequencies. This comparison of experimental and theoretical spectra revealed valuable details about the computational method's ability to characterise vibrational modes. The title compound has a dipole moment of 3.3514 Debye, which implies that it is polar. The nitrogen atom on oxadiazole ring was discovered to be the binding site for electrophilic attack using molecular electrostatic potential surface analysis. The energy difference between the HOMO, LUMO and global chemical reactivity parameters revealed that the compound is kinetically stable.

Acknowledgements

The Authors acknowledge the KTHM College, Nashik for FT-IR spectral analysis. The authors also would like to thank Principal of MGV's L.V.H. Arts, Science and Commerce College, Panchvati, Nashik for permission and providing necessary research facilities. Authors are also grateful to Ex Professor Dr. A. B. Sawant for Gaussian study. Dr. Aapoorva Prashant Hiray, Coordinator, MG Vidyamandir Institute, is gratefully acknowledged for Gaussian package.

Disclosure statement

No potential conflict of interest was reported by the authors.

ORCID

Sunil L. Dhonnar: 0000-0002-4098-3107

Vishnu A. Adole: 0000-0001-7691-7884

Nutan V. Sadgir: 0000-0002-7281-8376

References

[1] S.R. Pattan, P.A. Rabara, J.S. Pattan, A.A. Bukitagar, V.S. Wakale, D.S. Musmade, *Ind. J. Chem.*, **2009**, *48B*, 1453–1456. [CrossRef], [Google Scholar], [Publisher]

[2] J.N. Sangshetti, A.R. Chabukswar, D.B. Shinde, *Bioorg. Med. Chem. Lett.*, **2011**, *21*, 444–448. [CrossRef], [Google Scholar], [Publisher]

[3] P.R. Kagthara, N.S. Shah, R.K. Doshi, H.H. Parekh, *Ind. J. Chem.*, **1999**, *38B*, 572–576. [CrossRef], [Google Scholar], [Publisher]

[4] P. Sengupta, D. Dash, C.Y. Yeliger, K. Myrugesh, *Ind. J. Chem*, **2008**, *47B*, 460–462. [Google Scholar]

[5] A. Singh, M. Lohani, R. Parthsarthy, *Iran. J. Pharma. Res.*, **2013**, *12*, 319–323. [CrossRef], [Google Scholar], [Publisher]

[6] A. Almasirad, S.A. Tabatabai, M. Faizi, A. Kebriaeezadeh, *Bioorg. Med. Chem. Lett.*, **2004**, *14*, 6057–6059. [CrossRef], [Google Scholar], [Publisher]

[7] M. Amir, K. Saifillah, W. Akhter, *Ind. J. Chem*, **2011**, *50B*, 1107–1111. [CrossRef], [Google Scholar], [Publisher]

[8] S.L. Dhonnar, V.A. Adole, N.V. Sadgir, B.S. Jagdale, *Phy. Chem. Res.*, **2021**, *9*, 193–209. [CrossRef], [Google Scholar], [Publisher]

[9] A. Kumer, Md. N. Sarker, S. Paul, *Turk. Compu. Theor. Chem.*, **2019**, *3*, 59–68. [CrossRef], [Google Scholar], [Publisher]

[10] M. Islam, A. Kumer, N. Sarker, S. Paul, A. Zannat, *Adv. J. Chem. Sec. A*, **2019**, *2*, 316–326. [CrossRef], [Google Scholar], [Publisher]

[11] A. Kumer, S. Paul, M. Sarker, M. Islam, *Int. J. New Chem.*, **2019**, *6*, 236–253. [CrossRef], [Google Scholar], [Publisher]

[12] A. Kumer, N. Sarker, S. Paul, A. Zannat, *Adv. J. Chem. Sec. A*, **2019**, *2*, 190–202. [CrossRef], [Google Scholar], [Publisher]

[13] A. Kumer, M. Sarker, S. Paul, *Eur. J. Envi. Rese.* **2019**, *3*, 1–10. [Google Scholar], [Publisher]

[14] A. Kumer, M.Sarker, S. Paul, *Intern. J. Chem. Tech.* **2019**, *3*, 26–37. [CrossRef], [Google Scholar], [Publisher]

[15] S.L. Dhonnar, B.S. Jagdale, A.B. Sawant, T.B. Pawar, S.S. Chobe, *Der Pharma Chemica*, **2016**, *8*, 119–128. [Google Scholar], [Publisher]

[16] N.V. Sadgir, S.L. Dhonnar, A.B. Sawant, B.S. Jagdale, *SN Applied Sci.*, **2020**, *2*, 1376–1388. [CrossRef], [Google Scholar], [Publisher]

[17] S.L. Dhonnar , V.A. Adole , N.V. Sadgir , B.S. Jagdale, *Int. J. Res. Ana. Rev.*, **2019**, *6*(2), 674–682.

[18] V.A. Adole, R.H. Waghchaure, S.S. Pathade, M.R. Patil, T.B. Pawar, B.S. Jagdale, *Mol. Simul.*, **2020**, *46*, 1045–1054. [CrossRef], [Google Scholar], [Publisher]

[19] N.V. Sadgir, S.L. Dhonnar, B.S. Jagdale, B. Waghmare, *Mat. Sci. Res. India*, **2020**, *17*, 281–293. [CrossRef], [Google Scholar], [Publisher]

[20] S.S. Pathade, B.S. Jagdale, *Phys.Chem. Res.*, **2020**, *8*, 671-687. [CrossRef], [Google Scholar], [Publisher]

[21] P. Sjoberg ,P. Politzer, *J. Phys. Chem.*, **1990**, *94*, 3959–3961. [CrossRef], [Google Scholar], [Publisher]

[22] V.A. Adole, T.B. Pawar, B.S. Jagdale, *J. Sulphur Chem.*, **2021**, *42*, 131–148. [CrossRef], [Google Scholar], [Publisher]

[23] V.A. Adole, *J. Appl. Organomet. Chem.*, **2021**, *1*, 29–40. [CrossRef], [Google Scholar], [Publisher]

[24] V.A. Adole, *Adv. J. Chem. A,* **2021**, *4*, 175–187. [CrossRef], [Publisher]

[25] R.A. Shinde, V.A. Adole, *J. Appl. Organomet. Chem.*, **2021**, *1*, 48–58. [CrossRef], [Google Scholar], [Publisher]

[26] M.J.E.A. Frisch, Gaussian 03, Revision E.01, Gaussian, Inc. Wallingford CT, **2004**. [Google Scholar]

[27] A.D. Becke, *J. Chem. Phy.*, **1993**, *98*, 5648–5652, [CrossRef], [Google Scholar], [Publisher]

[28] C. Lee, W. Yang, R.G. Parr, *Phy.Review B*. **1988**, 37, 785–789, [CrossRef], [Google Scholar], [Publisher]

[29] J.B. Foresman, A.E. Frisch. *Exploring chemistry with electronic structure methods* (2nd Edn. Gaussian, Inc. Pittsburgh; PA), **1996**. [Google Scholar]

[30] R. Dennington, T. Keith, J. Millam, Gauss View, Version 4.1.2. Semichem Inc. Shawnee Mission, KS, **2007**. [Google Scholar]

[31] T. Koopmans, *Physica*, **1934**, *1*, 104–113, [CrossRef], [Google Scholar], [Publisher]

[32] R.G. Pearson, *J. Org. Chem*., **1989**, *54*, 1423–1430, [CrossRef], [Google Scholar], [Publisher]

[33] R.G. Parr, L.V. Sznetpaly, S.J. Liu, *J. Am. Chem. Soc.,* **1999**, *121*, 1922–1924, [CrossRef], [Google Scholar], [Publisher]

[34] P.K. Chattaraj, S. Giri, *J. Phy.Chem. A.,* **2007**, *111*, 11116–11126, [CrossRef], [Google Scholar], [Publisher]

[35] P.K. Chattaraj , S.U. Maiti, *J. Phy. Chem. A.,* **2003**, *107*,1089–5639, [CrossRef], [Google Scholar], [Publisher]

[36] M.M. Hoque, Md. S. Hussen, A. Kumer, Md. W. Khan, *Mol. Simul.*, **2020,** *46*, 1298–1307, [CrossRef], [Google Scholar], [Publisher]

[37] M.K. Ahmed, A. Kumer, A.B. Imran, *R. Soc. Open Sci.,* **2021**, *8*, 202056, [CrossRef], [Google Scholar], [Publisher]

[38] J. Aihara, *J. Phys. Chem. A.,* **1999**, *1033*(7) 7487–7495, [CrossRef], [Google Scholar], [Publisher]

[39] Ö. Mıhçıokur, T. Özpozan, *J. Mol. Struc*., **2017**, *1149*, 27–41. [CrossRef], [Google Scholar], [Publisher]

[40] Xavier, N. Rashid, I. Hubert Joe, *Spectrochimica Acta Part A: Mole. Biomole. Spectr.,* **2011**, *78*, 319–326, [CrossRef], [Google Scholar], [Publisher]

HOW TO CITE THIS ARTICLE

Sunil L. Dhonnar*, Nutan V. Sadgir, Vishnu A. Adole, Bapu S. Jagdale. Molecular Structure, FT-IR Spectra, MEP and HOMO-LUMO Investigation of 2-(4-Fluorophenyl)-5-phenyl-1, 3,4-oxadiazole Using DFT Theory Calculations. *Adv. J. Chem. A.*, **2021**, 4(3), 220-230.

DOI: 10.22034/AJCA.2021.283003.1254
URL: http://www.ajchem-a.com/article_130816.html